

Mapping connectivity in discontinuous metal films with a scanning tunneling microscope

V. Z. Chorniy and C. J. Adkins

Cavendish Laboratory, University of Cambridge, Madingley Road, Cambridge CB3 0HE, United Kingdom

(Received 24 October 1995)

We describe a method for mapping connectivity in discontinuous metal films on semiconducting substrates. A low-temperature scanning tunneling microscope was used to image connectivity in discontinuous gold films on GaAs(001). The method relies on the fact that gold on GaAs forms Schottky diodes, the resistance of which depends on the area. Larger groups of connected islands exhibit smaller resistance to the substrate at a given bias than smaller groups of islands. Current-imaging tunneling spectroscopy is used to display these changes.

Since the early 1960s connectivity and percolation processes in thin metal films have attracted considerable interest. Soon after the invention of the scanning tunneling microscope (STM) the technique of scanning tunneling potentiometry (STP) was developed; it provides information about the connectivity of films.¹⁻⁵ Unfortunately STP has serious drawbacks: STP requires changes to STM design, is prone to tip-surface artifacts, and most importantly, STP provides only one-dimensional information on connectivity along the direction of the applied field. Here we will demonstrate a truly two-dimensional approach, which eliminates these shortcomings and provides not only information about connectivity and related processes, but also offers possibilities for studies of thin film growth, and Schottky barrier physics, and could be complementary to a variety of other techniques such as ballistic-electron emission microscopy (BEEM).

The GaAs(001) used as a substrate was heavily doped with Si to ensure good conductance at low temperatures. The Si concentration was between 1.2×10^{18} and 2.3×10^{18} cm⁻³ according to the manufacturer's specifications. After cleaning the GaAs surface by a successive series of ion sputtering and annealing, a Au film of approximately 8 nm mean thickness was deposited in an MBE chamber under UHV conditions at a rate of approximately 1 pm s⁻¹ with a substrate temperature of 120 °C. The film was found to be discontinuous by resistivity measurements, but at this thickness it is expected to be close to the percolation threshold, which corresponds well with our STM observations. A general topographic image of the film is shown in Fig. 1. For our experiments we used a simple low-temperature scanning tunneling microscope. The STM had standard electronics and software, but was also fitted with an additional current amplifier, which allows the measurement of low resistances occurring at point contacts. For these experiments the STM head was mounted in a continuous-flow cryostat. A cut gold tip was used.

It is well known that Au on GaAs forms a Schottky diode.⁶ This was confirmed by bringing the STM tip into contact with the film and measuring current-voltage (*I-V*) characteristics at room temperature and at 3.5 K. For both temperatures, at forward bias (negative in our setting), the *I-V* characteristics exhibited a roughly exponential *I* vs *V* dependence, but a dramatic change in the range of resistance occurs at liquid-helium temperature. At both temperatures

the (full) forward bias resistance was small (of order 100 Ω), while the zero-bias resistance might typically rise from a few tenths of a MΩ at room temperature to GΩ at 3.5 K. The resulting tip indentations were later imaged by STM. Those made at room temperature had indentation diameters of about 1 μm and those made at 3.5 K had diameters of 0.1–0.3 μm. In order to follow standard semiconductor notation terms “larger” or “smaller” bias will refer to the absolute value of the forward bias.

During normal STM operation a tip is separated from a sample by a tunneling gap. Therefore the current measured by the STM is determined by the resistance of a tunneling junction R_t and the resistance of a diode R_d connected in series. The influence of the diode properties on STM behavior could be seen in the *I-V* characteristics and most dramatically in the *s-V* (tip height vs voltage at preset current) characteristics. Initially the *s-V* curve shows the normal weak dependence on voltage determined by tunneling through the gap, but as the diode resistance is being approached, the gap closes increasingly quickly and eventually the tip crashes into the surface.

As we have mentioned, the film is discontinuous, but we assumed it to be near the percolation threshold. (Gold films of this thickness grown at room temperature on insulating substrates are continuous.) We may therefore expect that this

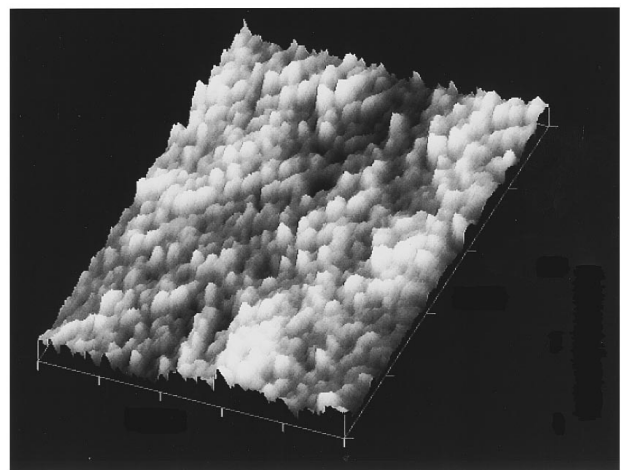


FIG. 1. General $1.5 \mu\text{m} \times 1.5 \mu\text{m}$ topograph taken at room temperature at +56 mV/1 nA. The vertical range is 29 nm.

film consists of gold islands, some of which are isolated from the rest and some of which are connected. The connected islands form a diode with larger area than an isolated island and therefore they should have a smaller R_d .

The shape of the I - V characteristic taken over a diode depends on its resistance (and therefore its area), provided that R_d is not much smaller than R_t at some part of the I - V curve. In particular, if R_d is comparable to R_t at the current and voltage at which the tip is stabilized (I_{stab} and V_{stab}), then the I - V characteristics taken over diodes of larger area will be more linear than those taken over small-area diodes. In other words, they show a larger current at a bias smaller than V_{stab} and smaller current at a bias larger than V_{stab} . Of course, all I - V characteristics pass through the origin and through $(V_{\text{stab}}, I_{\text{stab}})$. This difference in the characteristics is ideally suited for mapping by current-imaging tunneling spectroscopy (CITS). In this technique the tip is scanned across the film's surface to obtain a topographical image in standard constant current mode, but in addition, above each point of a scan the feedback is disabled to keep the gap constant, and the bias is ramped through preset values, i.e., an I - V characteristic is taken above each point of the film. For each of these voltages a current map is formed. If such a map is made at $V < V_{\text{stab}}$ at the settings described above, then isolated islands will show up as areas of relatively low current (dark) and groups of connected islands as areas of relatively high current (light). The reverse is the case for $V > V_{\text{stab}}$.

One should note that although the voltage is varied in the STM, current is the independent variable as far as R_d and R_t are concerned. We chose a current of 1 nA as the optimum setting for I_{stab} because, at this current, diodes in the film typically exhibit resistances of approximately 600 M Ω , which is close to the tunneling junction resistance used in the majority of STM experiments. This allows R_t to be set large enough for stable STM operation at the optimum contrast setting (see discussion below), and far enough from the maximum resistance of the diodes (G Ω). Of course, the question of the optimum setting for V_{stab} is equally important. For any bias V , the current measured above a film is $I = V/(R_d + R_t)$. Therefore, for better contrast, we need to set up our STM so that R_t is as small as possible. Firstly, a smaller R_t results in a higher current level on the current maps, which gives a better signal-to-noise ratio. Secondly, it gives the current maps better contrast. At the bias V at which the current map is taken, the ratio of current for small- and large-area diodes (I_s and I_l) will be given as

$$\frac{I_l}{I_s}(V) = \frac{R_{d,s}(I_s) + R_{t,s}(I_s)}{R_{d,l}(I_l) + R_{t,l}(I_l)}, \quad (1)$$

where $R_t(I)$ takes into account the nonlinearity of the I - V characteristics of tunneling. The nonlinearity we wish to use to generate the images is in R_d so that reducing R_t will increase the contrast ratio. If $R_t \ll R_d$ the contrast ratio, I_l/I_s , approaches the maximum possible value of $I_l/I_s(V) = R_{d,s}/R_{d,l}(V)$, but, if R_t is too small, stabilization of the gap becomes problematic.

In order to choose an optimum bias, large enough to prevent the tip from crashing during scanning but also small enough to make $R_t < R_d$, we initially explored the gap-

voltage (s - V) behavior at random points on the film and noted the bias (a) at which the gap begins to close rapidly and (b) below which I decreased with V , indicating contact between the tip and film. Done with care this procedure does not cause damage to the tip. As a result of this approach a bias of -700 mV was chosen as optimum. After the first successful CITS scan, I - V and s - V characteristics could be taken over the areas of largest resistance and V_{stab} could be fine tuned. In our case this readjustment was not necessary. However, dependence of the contrast ratio on R_t in accordance with Eq. (1) was verified experimentally by increasing V_{stab} above the optimum value.

Figures 2(a) and 2(b) show a topograph and CITS current map of the same area for this optimum setting. All presented images have been put through a low pass filter and the current maps are an average of four, taken consecutively during the same scan.⁷ The current map [Fig. 2(b)] displays a few dark (high resistance) areas corresponding to isolated groups of islands, surrounded by light areas of islands better connected to each other. Here we have a real-space two-dimensional image of percolation. As would be expected, it shows various degrees of connectivity mapped by different current levels, which can be seen in Fig. 2(b) and more conveniently on the corresponding line profile [Fig. 2(c)]. We can observe a range of currents with the lowest level coming from the single most disconnected island and the higher levels coming from better and better connected areas. The range of current in the map is approximately 70–110 pA. $R_d(I)$ and $R_t(I)$ dependencies can be extracted from individual I - V characteristics through their different current dependencies.⁸ The details of the extraction process will be discussed elsewhere. The resistance displayed by the most connected areas of film corresponds to $R_d \approx 3.1$ G Ω , and $R_t \approx 150$ M Ω with a current of 107 pA. This value of R_d is slightly larger than the resistance of 2.5 G Ω measured using a point contact as described earlier. Indeed, such a relationship should be expected, because the resistance of a point contact depends on indentation size: in our case the tip forms a contact with a few areas of film of different resistance, so point-contact resistance should probably be expected to be smaller than, but similar to, the value of the most conductive area of the film. Exact comparison is impossible because tip contact dramatically alters the geometry of the film.

One might ask why the measured current, and therefore resistance, varies only by a factor of roughly 2, given that the film is composed of diodes of greatly different areas. To answer this question we have to consider conduction mechanisms of the film in more detail. At a negative bias (which is a forward bias for our configuration) there are three conduction paths, and therefore three components, of the current. The first current component I_1 consists of electrons tunneling through the Schottky barrier (SB) in the field-emission regime⁹ from the semiconductor to the metal island (or group of electrically connected islands) above which the tip is positioned (we shall call it the “probed island”). The second component I_2 consists of electrons reaching neighboring islands and then tunneling from them to the probed island through the vacuum gap separating them. The third component I_3 consists of electrons reaching neighboring islands as in the second case, but tunneling to the probed island through the semiconductor substrate. Let us consider the last case

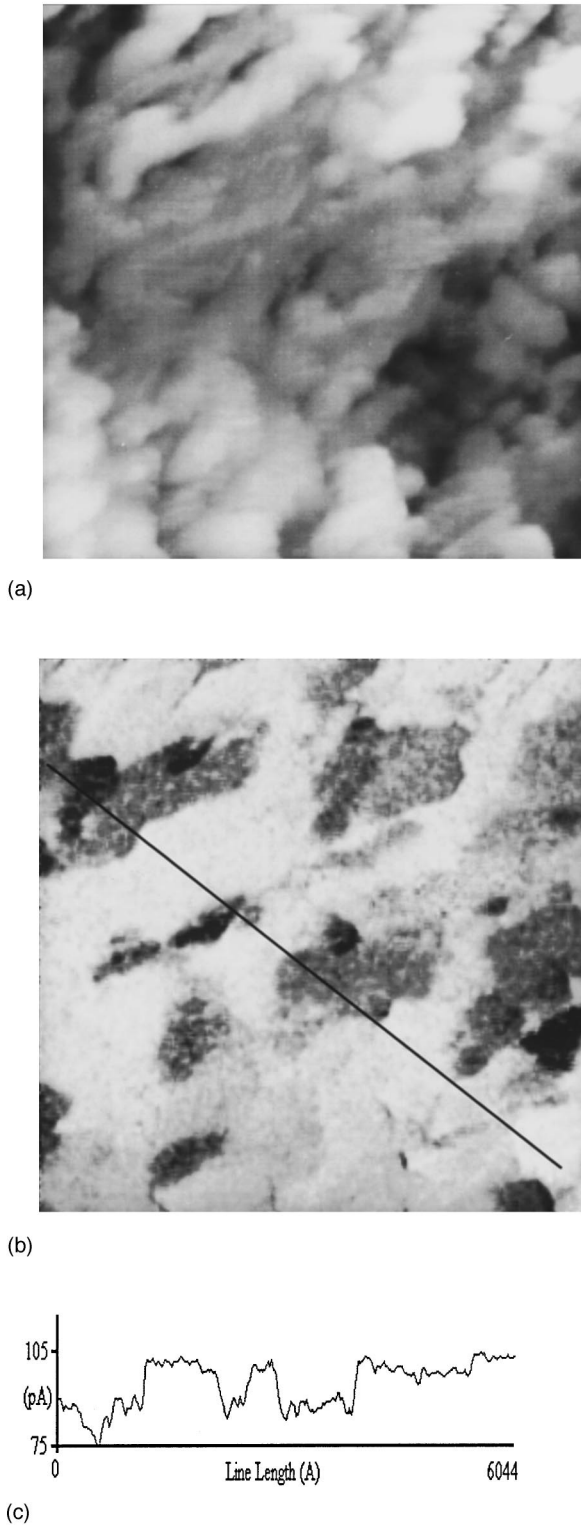


FIG. 2. All CITS images are for the same area, $500 \text{ nm} \times 500 \text{ nm}$, and were obtained at 3.5 K. (a) Topograph at $-700 \text{ mV}/1 \text{ nA}$. The vertical range is 9.4 nm. (b) Current map at -350 mV for $-700 \text{ mV}/1 \text{ nA}$ setting. (c) Line profile along the dark line on the current map of (b).

more closely. Assuming a donor concentration of $1.5 \times 10^{18} \text{ cm}^{-3}$, the depletion width w of the space-charge region can be estimated at low temperature as $w = \sqrt{2\epsilon_r\epsilon_0(\Phi - V_{\text{bias}})/N_d} \approx 23 \text{ nm}$, where ϵ_r is the relative

permittivity of GaAs at low temperature, Φ is the Schottky barrier height (SBH), N_d is donor concentration, and $V_{\text{bias}} = 350 \text{ mV}$. Obviously, if the separation l between islands of the film is a few nm, it is much smaller than the depletion width and electrons can tunnel from island to island through a potential barrier, which can be well approximated as a rectangular barrier with a height equal to SBH ($e\Phi$ is approximately 0.9 eV in our case¹⁰) and width l . Both interisland tunneling mechanisms (through vacuum and through semiconductor) depend on distance l . However, tunneling through the vacuum (component I_2) corresponds to a rectangular potential barrier of height roughly equal to the work function of the metal, which is approximately 5.4 eV for gold. Therefore $I_{2,3} \propto \exp(-2l\sqrt{2m\varphi_{2,3}/\hbar}) \approx \exp[-(l/\text{\AA})\sqrt{(\varphi_{2,3}/\text{eV})}]$, where $\varphi_2 = 5.4 \text{ eV}$, and $\varphi_3 = 0.9 \text{ eV}$. Variation in connectivity between the islands is determined by variation of $(I_2 + I_3)$. This component increases with the perimeter of a cluster.

The question of whether I_2 or I_3 dominates their sum and its variation due to changes of l would be obvious if the distance l were the same for both conduction paths. In fact, metal islands may have angles of contact with the substrate greater than $\pi/2$, making the distance between islands through the vacuum smaller than the distance through the semiconductor. As a result, in a film close to the percolation limit when distances between islands are small, I_2 can dominate the variation of $(I_2 + I_3)$. We believe this case applies to our film. This effect could provide information about the growth process. When “inward bending” of islands is significant, one could employ the STM to observe a change of current behavior when the average distance between islands becomes smaller than some critical value that will depend on the contact angle between semiconductor and metal.

Now we return to the first component I_1 , i.e., electrons flowing through the SB from the semiconductor to the probed island. If $w \geq l$ the semiconductor has a depletion region of almost uniform depth spreading underneath the entire film, edge effects are unimportant and the current I_1 through a diode is proportional to its area. If, on the other hand, $w \lesssim l$, tunneling to the substrate takes place more easily at the edge of an island because of the concentration of field lines. In this case, edge effects play an important role, and for diodes of small area it is found that the current scales with the perimeter rather than with area.¹¹ Inhomogeneities can also give rise to currents proportional to the perimeter.¹² All these factors act to reduce the magnitude of total current variations.

To ensure that I - V characteristics exhibited the expected behavior over all of the imaged area, we also took current maps at $+350 \text{ mV}$, which gave a picture similar to Fig. 2(b), and at -1000 mV , which gave the same picture in reverse contrast, i.e., “light” areas become “dark” and vice versa, as expected. These settings give less reliable maps of the connectivity as they allow the I - V characteristics to be more influenced by features unrelated to the diodes.

We should note that, since tip stabilization holds ($R_t + R_d$) constant (at V_{stab}) during a scan, the tip height above the surface changes with horizontal position because of changes in R_d . However, since the tip height depends logarithmically on R_t , typical variations of R_d cause negli-

gible changes in tip height under the settings actually used. [For example, in Fig. 2(a), R_t varied between approximately 50 and 150 M Ω with $R_t + R_d$ held at 700 M Ω .] We should also note that the comparison of these current maps with regular topographs yields additional information about morphology of the film, as they resolve the small gaps between islands, which are poorly observed or may not be observable at all in normal STM topography because of the finite size of the STM tip. This information is also two dimensional and provides subnanometer resolution similar to the one-dimensional information of STP images.^{2,3,5} In our work, the smallest measured distances between regions of different resistance was found to be less than 3 nm. Also, we should point out that our maps are not susceptible to the tip-surface convolution artifacts of STP, which introduce artificial potential discontinuities,^{3,4} because our CITS images are derived from current flow over the connected areas of the film (islands or groups of islands), which are relatively large in comparison to the tip.

Unfortunately our method could be subject to artifacts of another kind, however, due to SBH inhomogeneity. Generally speaking, our method forms maps of spatial variation of R_d and to extract direct information about connectivity one should have a map of variations of SBH, for example, a BEEM image. There are two reasons why the observed variations should be interpreted as connectivity maps. The first one is general: if these current variations are due to connectivity differences then the size of a connected area should correlate with the measured CITS current; i.e., larger areas should display more current. In the light of earlier discussion of the magnitude of current variations, we may assume that current levels would scale roughly with the perimeter of constant current areas. This is exactly what was observed. Such correlation would not be expected from variations of the SBH. The second argument is more specific and enforces the first one in relation to the particular setting of our experiment. Tung *et al.*¹² have shown that at low temperature the diode current will be dominated by low barrier height patches inside the diode. At liquid-helium temperatures, this means that one should be most aware of the largest

fluctuation in SBH. In BEEM images for GaAs the variations happen on nm scale, i.e., within the dimension of a single island, especially for low SBH patches.¹³ Thus, if fluctuations of SBH were responsible for our maps, they would have shown a random distribution of current levels associated with individual islands, not with large groups of them. Of course, a single isolated island on our connectivity map may be an artifact due to SBH inhomogeneities; however, one would then expect that, equivalently to single islands which show low current level corresponding to high barrier height, there should be a number of single islands showing a high current level corresponding to low barrier height; but this has not been observed. Thus, the observed current variations are unlikely to be connected with SBH inhomogeneity. Therefore the conclusion is that, although artifacts due to SBH inhomogeneity may be present, they are definitely not dominating.

In conclusion, we would like to say that although STP has previously yielded information about the connectivity of films, to the best of our knowledge, we have presented the first real-space map of connectivity in a discontinuous metal film. Our approach may be used for various degrees of metal coverage. A study of such images, obtained over large areas, would provide important experimental evidence about percolation processes, which is the subject of numerous theoretical and computer simulation studies. Unfortunately, our STM design does not allow sample movement in the x - y plane during experiment, which limits the size of the mapped area. On a smaller scale, CITS images of films of different thickness in combination with data from I - V and s - V characteristics carried out under different conditions do allow us to extract additional information about the properties of the interfaces, small-area diodes, and various edge effects. The results will be reported in future papers.

The authors are grateful to Simon Gray for sample preparation, and acknowledge the technical support of WA Technology and financial support of VZC through the Committee of Vice-Chancellors and Principal's Overseas Research Student Scheme, and by the Cambridge Overseas Trust and the Taylor Fund.

¹P. Murali *et al.*, IBM J. Res. Dev. **30**, 443 (1986); P. Murali and D. W. Pohl, Appl. Phys. Lett. **48**, 514 (1986).

²J. R. Kirtley *et al.*, Phys. Rev. Lett. **60**, 1546 (1988).

³A. D. Kent *et al.*, J. Vac. Sci. Technol. A **8**, 459 (1990).

⁴J. P. Pelz and R. H. Koch, Phys. Rev. B **41**, 1212 (1990).

⁵J. Besold *et al.*, Appl. Surf. Sci. **65/66**, 23 (1993).

⁶S. M. Sze, *Physics of Semiconductor Devices*, 2nd ed. (Wiley, New York, 1981).

⁷Each map is separated from the next by approximately 350 μ s. Comparison between the first and the last maps shows only minor differences, which proves that the variations of current level on the maps are not caused by charging of disconnected metal islands and Schottky diodes. (The R - C time constant of a typical island is estimated to be much smaller than 1 ms.) In addition, the fact that the contrast ratio of the connectivity maps follows Eq. (1) also testifies against charging as a possible cause.

⁸The separation of $R_d(I)$ and $R_t(I)$ was based on fitting the data, using the fact that $R_t(I)$ is almost constant near V_{stab} , I_{stab} , while $R_d(I)$ has the typical nonlinear diode form in 0–10 nA range (verified by “gentle” point contacts as in a search for optimum settings).

⁹F. A. Padovani and R. Stratton, Solid State Electron. **9**, 695 (1966).

¹⁰E. H. Rhoderick and R. H. Williams, *Metal-Semiconductor Contacts* (Clarendon, Oxford, 1988), p. 70.

¹¹P. A. Tove *et al.*, Solid State Electron. **16**, 513 (1973); D. Dascalu *et al.*, *ibid.* **24**, 897 (1981); J. P. Sullivan *et al.*, J. Vac. Sci. Technol. A **10**, 1959 (1992).

¹²J. P. Sullivan *et al.*, J. Appl. Phys. **70**, 7403 (1991); R. T. Tung *et al.*, Mater. Sci. Eng. B **14**, 266 (1992); R. T. Tung, Phys. Rev. B **45**, 13 509 (1992).

¹³M. Prietsch, Phys. Rep. **253**, 163 (1995), and references therein.